Academic Journal of Research and Scientific Publishing | Vol 4 | Issue 45
Publication Date: 5-1-2023 ISSN: 2706-6495

Crystallites Dimensions and Electrical Conductivity of Solid Carbon Pellets (SCPs) from Date Palm Leaves (Phoenix dactylifera L.)

Author: Dr. Abubaker Elsheikh Abdelrahman

Associate Professor, Director of Act Center for Research, Singa, Sudan

*Corresponding Author Email: abuelsheikh76@gmail.com

Co-Author: Dr. Fatima Musbah Abbas

Assistance Professor, Biology Department, Faculty of Science, King Khalid University, Saudi Arabia

Email: fmelamin@kku.edu.sa

Co-Author Dr. Selma Elsheikh Abdelrahman

Assistance Professor, Director of computer programs and Training Act Center, Singa, Sudan

Abstract

Solid carbon pellets (SCPs) were prepared from self-adhesive properties of date palm leaves (*Phoenix dactylifera L.*), primary pre-carbonized at low temperature, milled to fine grain, powdered, and pelletized as a grain pellet by applying of (5-21) metric tons of compression load, to carbonization at 1000 ºC. The SCPs produced were analyzed in terms of the volume shrinkage, carbon yield, crystallites dimensions and electrical conductivity of the solid carbon pellets as a function of compression load. The values of the electrical conductivity were further analyzed in terms of percolation theory to estimate the critical density of the SCPs produced. The results show that the volume shrinkage and carbon yield after carbonization were in a range of 54.0-64.8% and 26.98-32.4%, respectively, indicating that the body is physically shrinking to maintain its structural integrity. X-ray diffraction intensity shows that the structures of the SCPs are non-graphitic, and their crystallite dimensions are improved by increasing the compressive load. The d_{002}, L_c and L_a data were found to obey the linear relation of d_{002} versus 1/ L_c and 1/ L_a, as L_c and L_a approach infinity. The electrical conductivity was varied with the compression load and 19 metric tons is a higher value than the others. The critical density of the SCP obtained from the percolation theory was 0.025 g/cm^3.

Keyword: Date palm leaves, grain pellets, carbon pellets, volume shrinkage, carbon yield, crystallite dimensions, electrical property, critical density.

1. Introduction

Carbon materials have attracted great attention in the last decade because of their numerous applications, such as electrical carbon brush (Tang et al., 2005), super capacitor (Pandolfo and Hollenkamp, 2006), electrochemical capacitors (Inagki et al., 2010), catalyst and catalyst support (Lam and Luong, 2014), and double layer capacitors (Arof et al., 2012).Carbon material has been made using a wide range of raw materials: biomass, petroleum coke, rank coals, bio-pitch, bio-oil, polymer in different forms powder, granular and pellets without or with filler reinforcements (Aso et al., 2004; Chunlan et al., 2005; Saeed et al., 2010, Dhyani and Bhaskar, 2018; Zhang et al., 2019; Lu et al., 2020; Wang et al., 2020) The pellet form is particularly useful because it is dense or contains particle sizes closed together in a solid manner. In addition, the shape of pellet form can provide a more fundamental understanding of the physical properties of carbon and the interactions that occur at its surface (Fatima et al., 2022). Several biomass materials have been tested to prepare carbon materials such as shells of mata kucing (*Dimocarpus longan*) fruit (Arof et al., 2012), cellulose (Adinaveen et al., 2016), date palm stones (Ahmed, 2016), oil palm wastes (Rashidi et al., 2017), lignocelluloses (Gonzalez, 2018) and date palm leaves (Fatima et al., 2022), found to be chemically stable in the environment. Frequently, it required careful preparation to improve it is physical and electrical properties and application. For example, the addition of metal material to improve it is electrical and mechanical properties (Kercher and Nagle, 2002; Deraman et al., 2004; Yan et al., 2016).

Characterization of the carbon structure can be made in terms of crystallite dimensions (d_{002}, L_c, and L_a) of the graphitic-like structure that are randomly distributed and oriented throughout the sample. Small graphitic-like structures reflect to disorder a structure which is sensitive to higher porosity content (Benedetti et al., 2018). It is well established in carbon materials that the mechanical properties of the carbon fibers are improved by increasing the crystalline and orientation, by electing a highly oriented precursor and then maintaining the initial high orientation during the carbonization process (Fatima et al., 2022). the electrical conductivity of carbon pellets prepared from oil palm empty bunch increased with the increasing molarities of nitric acid (HNO_3) (Deraman et al., 2002). Additionally, for the petroleum coke and graphite, it has been found the electrical conductivity and bulk density increased with increasing heat treatment temperature (Kim, 2001).

In the present work, the date palm leaves are being used for preparing solid carbon pellets because they're abundant, can be collected in a large amount and have low ash content. Primary, palm leaves were pre-carbonized at low temperature, milled into fine grain powder to improve its self-adhesive properties (Deraman et al., 2004), before being converting into a pellets by applying different compression load without adding any binder The objective of this work is to preparation solid carbon from date palm leaves by compression load, and attempt to establish various relationships between volume shrinkage carbon yields, crystallite size sand electrical conductivity of the solid carbon pellets as a function of compression load. The results of electrical conductivity were analyzed in term of percolation theory the estimate a critical density threshold. An X-ray diffraction programs is also applied to estimate the crystallite dimensions.

2. Material and Methods

Date palm leaves were pre-carbonized at 280 °C in a vacuum chamber for 4 hours, to cause them to shrink and break the date palm leaves microstructure, followed by ball milling for 20 hours milling time to produce a fine grain powder. About 2g of each grain powder was pelletized as a grain pellet by applying of 5, 7, 9, 10, 11, 12, 13, 14, 15, 17, 19 and 21 metric tons of compression load (354.175×10^4 N m^{-2}) in a mold of 2.75 cm diameter. These grain pellets were carbonized up to1000 ºC in a nitrogen environment using a multi-step heating profile (VulcanBoxFurnace3-1750). Programmed as1ºC/min from room temperature to 375 ºC where it was held for 1 hour before heating was resumed at 3 ºC/minto 800 ºC and then 5 ºC/min to 1000 ºC, where it was finally held for 5 minutes. Then system was automatically allowed to cool down naturally to room temperature.Then washed thoroughly with hot distilled water to remove the impurity and dried at 100 ºC for 2 hours. Results are given as the average from 5 replicates of each sample and analyzed as a function of compression load (CL) at room temperature. Measurements of the pellets dimensions before and after carbonization were carried out using a micrometer and the bulk density was determined by dividing the weight of the sample with its volume. The percentage of volume shrinkage and the carbon yield was calculated from the volume and the weight of the samples before and after carbonization.

Selected ACP samples were crashed into powder and mixed with KBr and compacted to form thin pellets.

The FTIR spectra were collected using a RFX-65 spectrophotometer capable of a maximum resolution of 0.12 cm^{-1} and equipped with an MCT liquid nitrogen-cooled detector, interferometer, detector and computer software, (model-KVB/Analects, INC). Infrared spectra were collected by using 2 to 5 milligrams (mg) of sample in a potassium bromide (KBr) pellet. The measurement was carried out using the Perkin Elmer System 2000 Fourier Transform Infrared (FTIR) with a pulsed laser carrier and a deutera-tedtriglycine sulfate detector. All the CPs were scanned from 400 to 4000 (cm^{-1}), with averaging 10 scans at 1.0 cm^{-1} intervals with a resolution of 0.25 cm^{-1}.

The XRD diffraction intensity of the CPs was analyzedusing (Bruker Advanced Solution AXS D8) equipment, with Cu K_α radiation and 1.5406 Å wavelength (λ). The pellets were scanned at 2θbetween 10º and 60º, with a step size of 0.04°. The diffraction intensity was corrected for the instrumental line broadening (Andrew and Dennis, 2002).Then diffraction intensity profiles recorded were fitted into a symmetrical Gaussian distribution. The crystallite dimensions (L_a, L_c) of the graphite-like crystallites can be calculated from the diffraction intensity using the Sherrier equation (1) and Warren's correction for the instrumental line broadening, by using Trace 1.4 programVarian 5 from Diffraction Technology PTG LTD, Australia. This program refines the intensity of each peak (as a separate variable) smooth the peak shape, as well as subtracts the background line and eliminates the $K\alpha_2$-peak from the diffraction intensity.

$$L_{c,a} = \frac{K\lambda}{\beta_{c,a}\cos\theta} \qquad (1)$$

where θ is the scattering angle position, K is a shape factor which is equal to 0.9 for L_c and 1.84 for L_a, $\beta_{c,\,a}$ *is* the width of a reflection at half-height expressed in radians. The relationships between d_{002}, L_c and L_a can be deduced by assuming a well known condition that for large L_a and L_c, ($\frac{1}{L_c}$ and $\frac{1}{L_a}$) approaches zero, then d_{002} versus($\frac{1}{L_c}$ and $\frac{1}{L_a}$) should follow a linear equation given as (Abubaker et al., 2006, Fatima et al., 2022)

$$d_{002} = \alpha_1 + \frac{\alpha_2}{L_a} \qquad (2)$$

where α_1 =3.354 Å is the interlayer spacing of pure graphite and α_2 is a constant (e.g., = 9.5 for L_a).

DC electrical conductivity (σ) was measured using the four-point-probe equipment (Keithley Micro-Ohmmeter) and the electrical conductivity (σ) given as:

$$\sigma = \frac{d}{RA} \quad (3)$$

Where d is the sample thickness, R (Ω) is the electric resistance and A is the area of the sample. First, the carbon samples were polished both sides, second, the electrical conductivity of graphite was used as the standard value to verify the accuracy of the measurement. The obtained results of were analyzed in terms of the percolation theory threshold above critical density (ρ_c) (Chunsheng and Yiu, 2008) given as

$$\sigma \sim (\rho - \rho_c)^t \quad (4)$$

where ρ is the bulk density, ρ_c is the critical density and τ is the power constant (~2) for the three dimensional. By plotting of log σ versus log (ρ-ρ_c) for $\rho > \rho_c$ for various values of ρc leads in every case to a straight line, with the slope of t.

3. Results and Discussions

3.1. Volume Shrinkage

The palm leavesis the lignocelluloses composed of cellulose, hemicelluloses and lignin as mean products. The weight loss was attributed to lignin and hemicelluloses firstly, decomposed at lower temperature and finally cellulose decomposed reasonably at 360 ºC in terms of moisture, tar, and gases, such as H_2, CO_2, CO, and O_2 (Dhyani and Bhaskar, 2018). Table 1, summarized the data of the solid carbon pellets before and after carbonization process. The bulk solid density increased but the apparent density decreased slightly after carbonization despite losing considerable weight and significant volume shrinkage. Similar behavior for carbon pellets from oil palm materials (Deraman et al., 2002) and cotton cellulose (Abubaker et al., 2006).

The volume shrinkage of the carbon pellets decreases with increasing compression load and becomes saturated at a higher CL.

This indicates that the compression load in the grain powder has an intrinsic tendency to reduce the volume shrinkage of the carbon pellets during the carbonization process due to squealing the particle size together in a solid manner.

3.2. Carbon Yields

Table 1 show the total yield of the carbonization process decrease at lowered load and further fluctuated at higher compression loads in a range of 26.98-32.4%, which is found similar to those of biomass olive stones treated with phosphoric acid (Yakout and Sharaf El-Deen, 20016). 5 metric tons of compression loads is exhibit a higher yield than the others.

Table 1: Metric Tons, Thickness (T_1, T_2), Diameter (D_1, D_2), bulk Density (ρ_1,ρ_2), volume shrinkage % and carbon yield % of the solid carbon pellets, before and after Carbonization

Grain Pellets				Solid Carbon Pellets				
Metric Tons	T_1 (mm)	D_1 (mm)	ρ_1 (g/cm^3)	T_2 (mm)	D_2 (mm)	ρ_2 (g/cm^3)	VolumeShrinkage %	Carbon Yield %
05	0.275	2.707	1.2439	1.99	19.60	1.063	64.8	32.40
07	0.264	2.716	1.3452	1.82	19.57	1.072	54.6	27.29
09	0.258	2.717	1.408	1.77	19.51	1.124	54.0	26.98
10	0.253	2.712	1.4669	1.79	19.45	1.212	59.3	29.66
11	0.251	2.703	1.4954	1.81	19.37	1.222	60.9	30.45
13	0.25	2.707	1.5051	1.80	19.37	1.293	63.7	31.87
14	0.248	2.71	1.5278	1.79	19.38	1.256	61.3	30.63
15	0.247	2.704	1.5436	1.77	19.34	1.281	61.0	30.48
16	0.246	2.714	1.5505	1.79	19.41	1.244	60.8	30.38
17	0.245	2.71	1.5654	1.77	19.38	1.298	61.9	30.95
19	0.244	2.712	1.5771	1.79	19.39	1.323	64.6	32.28
21	0.244	2.709	1.5789	1.77	19.37	1.276	60.8	30.41
SIG-K						1.540		
a								31-36.8

Note: SIG-K (Sigradur K) (Deraman et al. 2002) [a]is the carbon from the olive stones (Yakout and Sharaf-Ei-Deen 2016).

3.3. FTIR

For the SCPs treated from 5 to 21 metric tons of load, the spectra showed a broad band at 1652 cm-1 due to C=C stretching by the aromatic rings (Jia and Aik 1999) or it may be caused by the C=O stretching vibration of carboxyl or carbonyl groups. The band at 2950 cm-1 represents -CH stretching in the olefins or acetylene rings. For KOH treatment above 10 CLM, the FT-IR transmission spectra did not show any stretching band. Possibly, the carbon samples had a more amorphous structure, increasing the bond angle sufficiently to have had bands in slightly different positions from those in the crystalline phase. Otherwise, it reflects a homogenous structure in the carbon grain particles when it was prepared by a higher CL.

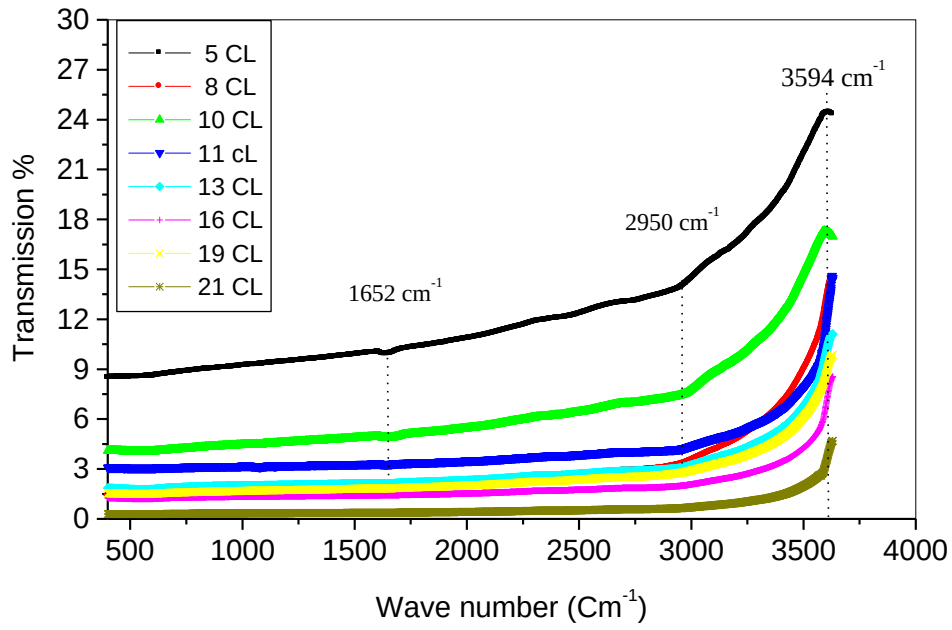

Figure 1: FTIR D of the solid carbon pellets

3.4. X-Ray Diffraction and Crystallite Dimensions

Figure 2 shows the X-ray diffraction of SCP contains two broad diffused at (002) and (100) peaks in roughly the same position as the peaks of pure graphite, results in a non-graphitic carbon structure (Song et al., 2011; Kristin et al., 2014). Similar observations have been shown on carbon -based petroleum coke (Lu et al., 2010). The order in the crystal is usually both positional and oriented, in that the molecules are constrained both to occupy specific sites in the lattice and to orientate their molecular axes in specific directions.

The diffraction intensity has been corrected to the background line, and instrumental boarding, and then fitted into the Lorentz distribution curve, as shown in Figure 3. As the diffraction profile overlaps and consists of four broad incomes peak, i.e., (002), (100) and (004), located at approximately 24.2°, 43.59°, and 52.0° diffraction angles, respectively. After correction, the diffraction intensity and Bragg's peaks were the same as in a graphite-like structure, and the layer separation was slightly further apart than in a graphite structure as shown in Figure 3.

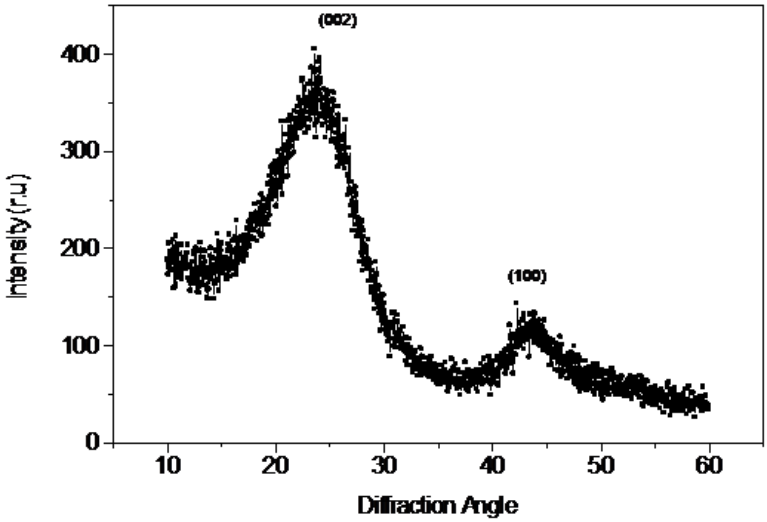

Figure 2: XRD intensity of solid carbon pellets

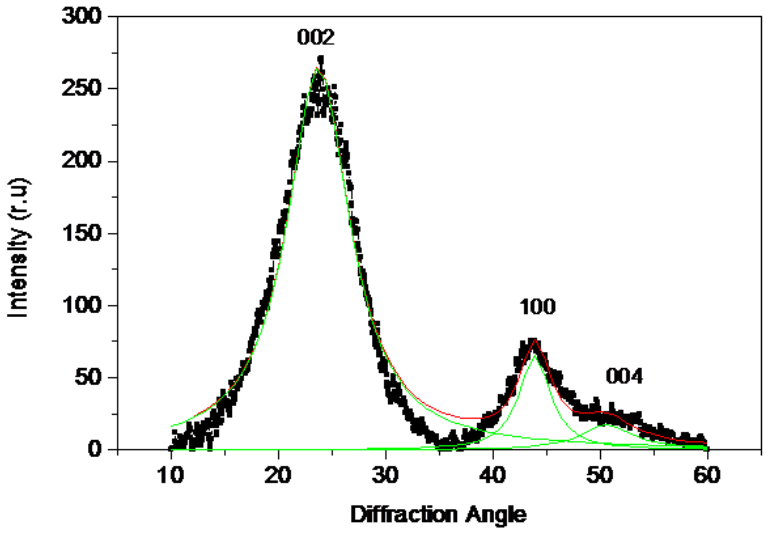

Figure 3: XRD intensity corrected to background line and fitted to Lorentz distribution curve

The d_{002} spacing of the carbon pellets produced is larger than that of graphite (i.e., d_{002} = 3.354 Å), reflecting the lower ordered structure. Also, d_{002} decreased with increasing compression load, indicating that a higher pressure gives a more crystalline structure as a consequence of the decreasing decrease in the d_{002}spacing of the SCPs produced as shown in Figure 4 and Table 2. The result also showed that both the L_c and L_a increased rapidly with increasing compression load from 5 to 12 metric tons of compression load, indicating an improved crystalline structure in the SCPs. Therefore, 16 tons of load gave the highest values of L_c and L_a, indicating that this pressure was sufficient for pelletizing grain powder. Above 16 metric tons, the values fluctuated, probably due to stress behavior at a higher compression load used for the pelletizing (Figure 5). This finding indicates that the compression load used for the pelletizing improved the crystalline dimensions of the SCPs produced.

From the data in Table 2, the values of d_{002}, L_c and L_a were compared to those of carbon made from phenanthrene and carbon from polyvinyl chloride (PVC) (Aso et al., 2004), carbonized at the same temperature, i.e., 1000 ºC. The values of L_c and d_{002} are in good agreement but L_a is lower than the values reported previously (Aso et al., 2004). The crystallite parameters of carbon samples, i.e. (d_{002}, L_c and L_a) were observed to increase with increasing CL.

Table 2: Crystallites parameters (L_c, L_a, d_{002}) and the electric conductivity of the SCPs

Metric Tons	**L_c (Å)**	**L_a (Å)**	**d_{002} (Å)**	**σ (Ω. $m^{)-1}$ X 10^5**
05	15.5	27.14	3.70	0.172
07	16.3	27.94	3.69	0.174
09	17.3	29.69	3.67	0.184
10	17.9	30.65	3.66	0.202
11	17.1	29.69	3.67	0.204
13	16.3	27.94	3.69	0.219
14	17.9	30.65	3.66	0.211
15	16.8	28.79	3.68	0.216
16	18.0	31.67	3.65	0.208
17	16.3	27.94	3.69	0.220

19	17.4	30.65	3.66	0.225
21	16.1	29.69	3.67	0.215
PVC-1000	16.0			-
AC-Type H		32	3.60	-
AC		27.57	3.70	
graphite		-		1

Note: PVC-1000 is for carbon precursor Polyvinyl chloride (PVC) (Aso et al. 2004) carbonized up to 1000 ºC. Activated carbon (AC) from cotton cellulose (Abubaker et al., 2006), AC-Type H is the commercial activated carbon (Saeed et al., 2014)

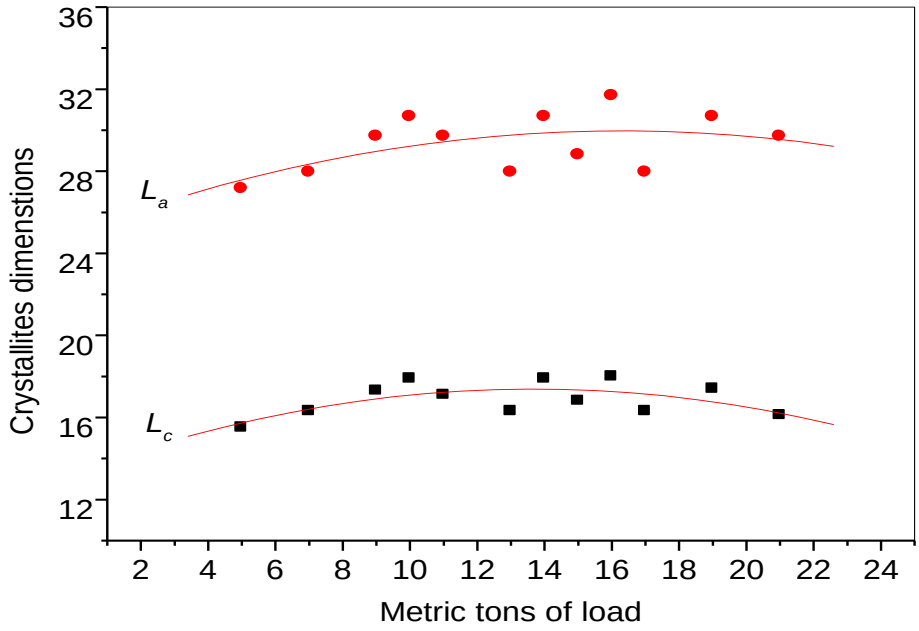

Figure 4: crystallites dimensions (L_a and L_c) versus CL

Our analysis of the d_{002} versus L_c and L_a was also found that obeyed the linear relation of d_{002} versus 1/ L_c and 1/ L_a, where d_{002} approached the value for pure graphite as L_a approaches infinity as shown in Figures 4 and 5. The linear equations are given as the following:

$$d_{002} = 3.342 + \frac{5.62}{L_c} \quad (5)$$

$$d_{002} = 3.354 + \frac{9.8}{L_a} \quad (6)$$

This linear correlation indicated that an improvement in the crystallite dimension occur simultaneously with the increase of L_a.

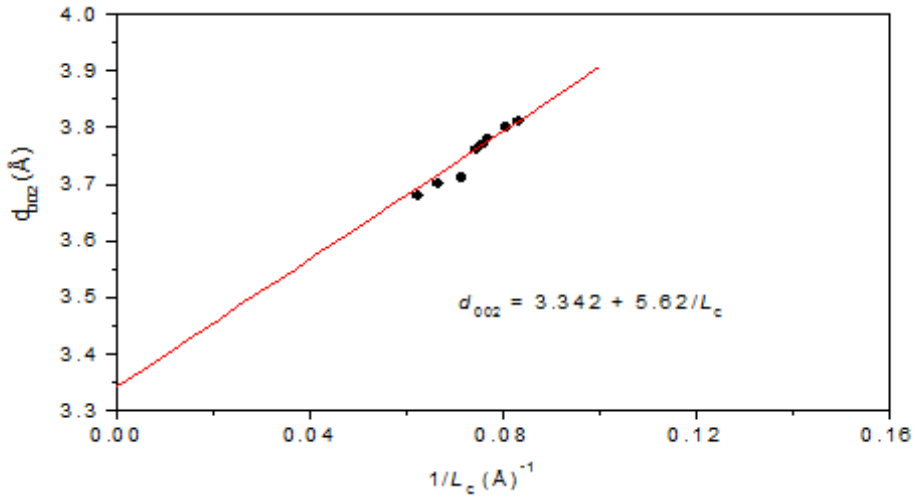

Figure 5: d_{002} versus $1/L_c$

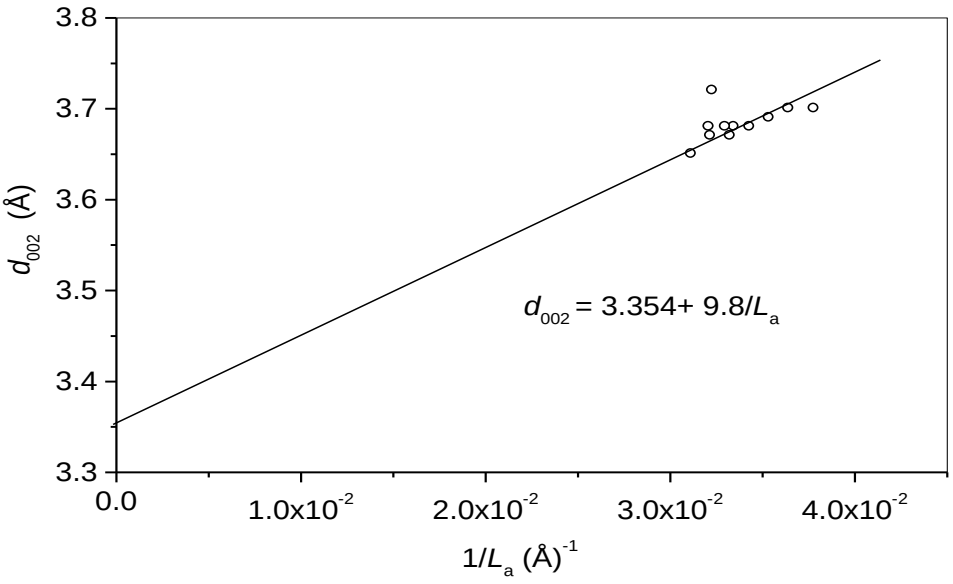

Figure 6: d_{002} versus $1/L_a$

3.5. Electrical Conductivity

The plot of electrical conductivity of the SCPs versus compression load is shown in Figure 6. The data in this figure show that the electrical conductivity of carbon pellets slightly increased with the increase of compression and exhibited its higher value at 19 tons pressure and then decreased. The increases in electrical conductivity are expected due to an improvement in its microstructure or preferred orientation. The electrical conductivity of the SCPs is less than that of a standard value of (SIG-K). This can be explained by the fact that during carbonization the volatile component is the interlayer's distance and pore size of the CPs, which reduces the amount of solid to conduct electrons. Or it's probably because of volatile organic matter microcrystalline, and more or less hydrated in organics substance (ash) may be considered as an insulating material.

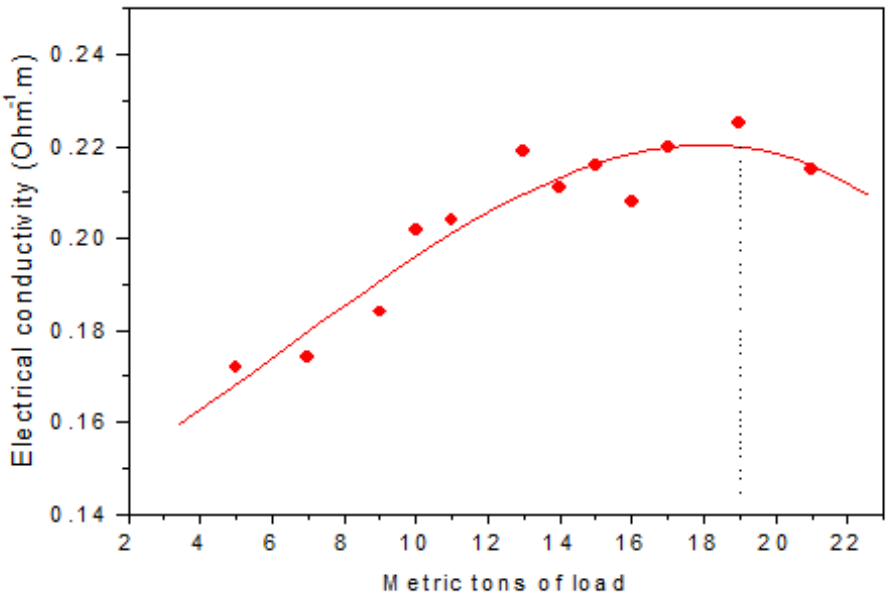

Figure 7: Electrical conductivity versus CL

3.6. Percolation Theory

The electrical conductivity is based on percolation theory, corresponding to the ACPs whose densities are located above its critical density ($\rho > \rho c$) by fitting log σ versus log ($\rho - \rho c$). This fitting was made by varying the values of ρc until the best linear curve fit is obtained, with the slope of 1.21 which is lower than the accepted universal value of $t \sim 2$ (Chunsheng and Yiu, 2008).

The intercept at the y-axis is 1.23, and the fitting value of ρc was found to be 0.025 g cm^{-3}, which represents the percolation threshold (critical density) for SCPs produced. This value is half of the percolation threshold of the graphite backbone (i.e., 0.05 g cm^{-3}) measured by Celzard et al., (2002). As follows from Table 2, the percolation theory was found to have a good correlation with the bulk density of the carbon samples, and it was interpreted by the increase in the bulk density of the carbon samples above 0.025 g cm^{-3}.

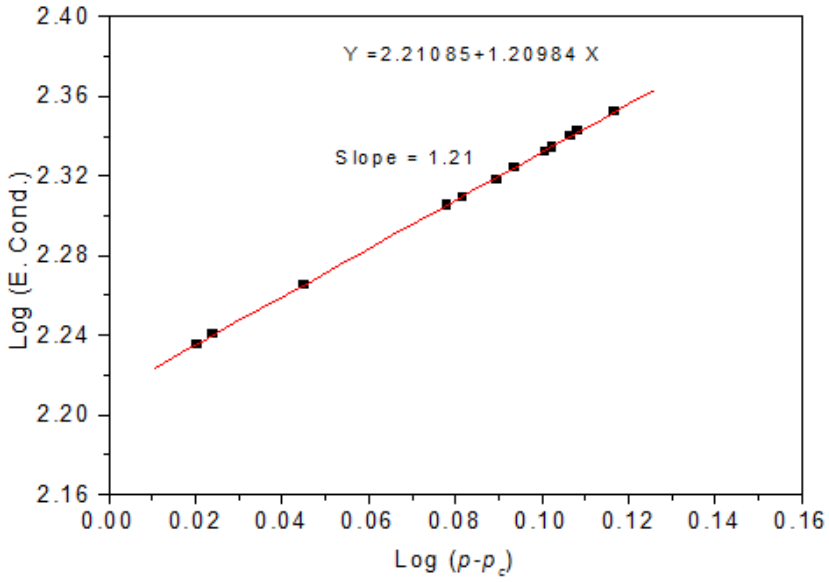

Figure 8: log (E. cond.) versus log (p-p_c)

Table 3: bulk density (p), electrical conductivity (σ), Log (σ) and Log (p-pc)

p (g/cm^3)	σ(Ω.cm)$^{-1}$	Log (σ)	Log(P-P_c)
1.063	172	1.2355	0.0204
1.072	174	1.2406	0.0241
1.124	184	1.2648	0.0449
1.212	202	1.3054	0.0781
1.222	204	1.3096	0.0817
1.293	219	1.3404	0.1065
1.256	211	1.3243	0.0938
1.281	216	1.3345	0.1024
1.244	208	1.3181	0.0896

1.298	220	1.34242	0.10823
1.323	225	1.35218	0.11661
1.276	215	1.33244	0.10072

4. Conclusion

The volume shrinkage and carbon yield reasonably varied with the compression load. FTIR data above 9 metric tons of compression pressures did not show any absorption band indicated non-carbon components had been released, forming a solid sample with a uniform structure. The crystallite dimensions of the carbon pellets (d_{002}, L_c and L_a) were observed to increase and decrease with increasing compression load. Also, increasing compression load increases the electrical conductivity of the carbon pellets produced, up to 19 metric tons of compression load. Justifying, thatan improvement in the inter-particle bonding,and more free carriers are created due to sequels the particle size together in asolid manner. The percolation theory found that 0.025 g/cm^3 is the critical density of the solid carbon pellets produced.

5. Acknowledgements

The authors extend their appreciation to Deanship of Scientific Research at King Khalid University for funding this work through General Research Project under grant number (GRO/323/43- 1443).

6. References

Abubaker E. A., MohamadD., SaraniZ., MohdH.J., Ramli O.,Astimar A. A., Mazliza M. and Rozan M. Y. (2006). Thermal and structural parameters analysis of carbon pellets prepared from KOH treated pre-carbonized cotton cellulose. J. Solid St. Sci. Technology Letters 13(1, 2): 39-47.

Aso, H., Matsuoka, K., Sharma, A. and Tomita, A. (2004). Structural analysis of PVC and PFA carbons prepared at 500-100 □C based on elemental composition, XRD and HRTEM. Carbon 42(12): 2963-2973.

Adinaveen, T., Judith, J. and John, L. (2016). Comparative Study of Electrical Conductivity on Activated Carbons Prepared from Various Cellulose Materials. Arabian Journal for Science and Engineering, 41:55–65.

Ahmed, M. J. (2016). Preparation of activated carbons from date (Phoenix dactylifera L.)palm stones and application for wastewater treatments: Review. Process Safety and Environment Protection, 102, 168–182.

Arof, A. K, M. Z. Kufian, M. Z, Aziz, Z. F., Abdelrahman, A. E. and Majid, S. R. (2012).Electrical double layer capacitor using Poly (methyl-methacrylate) - C4BO8Ligelpolymer electrolyte and carbonaceous material from shells Mata Kucing) Dimocarpuslongan)fruit. ElectrchimicaActa, 74:39-45.

Benedetti, V., Patuzzi, F, and Baratieri, M. (2018). Characterization of char from biomass gasification and its similarities with activated carbon in adsorption applications. Applied Energy, 227:92-99.

Celzard, A., Krzesinska, M., Begin, D., Mareche, J.F., Puricelli, S. andFurdin, G. (2002). Preparation, electrical and elastic properties of new anisotropic expanded graphite-based composites. Carbon, 40(4): 557-566 .

Chunlan, L., Shaoping, X., Yixiong, G., Shuqin, L. andChanghou, L. (2005). Effect of pre-carbonization of petroleum cokes on chemical activation process with KOH. Carbon, 43(12): 2295-2301.

Chunsheng L. and Yiu W. M. (2008). Anomalous electrical conductivity and percolation in carbon nanotube composite. J. Mater. Sci., 43:6012-6015.

Deraman, M., Omar, R., Zakaria, S., Mustapa I.R., Talib, M. and Alias, N. (2002). Electrical and mechanical properties of carbon pellets from acid (HNO3) treated self-adhesive carbon grain of oil palm empty fruit bunch. Journal of Mat. Sci. 37: 3329-3335 .

Deraman, M., Omar, R., Zakaria, S., Talib, M., Mustapa I.R., and Azmi, A. (2004). Hardness and microstructure of carbon pellets from self-adhesive pyro-polymer prepared from acid an alkaline-treated oil palm bunch. Advance in polymer technology, 23(1): 51-58 .

Dhyani, V. and Bhaskar, T. (2018). A comprehensive review on the pyrolysis of lignocellulosic biomass. Renewable Energy, 129:695-716.

Fatima M. A., Zehhba A. A., Rehab O. E. and Abubaker E. A. (2022). Characterization of carbon pellets prepared from date palm leaves (Phoenix dactylifera L.) by compression pressure: X-ray diffraction measurements and applications. Mol. Bio., 11(12):352.

Gonzalez G. P., (2018). Activated carbon from lignocelluloses precursors: A review of the synthesis methods, characterization techniques and applications. Renewable and Sustainable Energy Reviews, 82:1393-1414.

Inagaki, M., Konno, H. and Tanaike, O. (2010). Carbon materials for electrochemical capacitors. J. Power Sources 195:7880-7903 .

Jia G and Aik C.L. (1999). Textural and chemical characterizations of activated carbon prepared from oil-palm stone with H2SO4 and KOH impregnation. Journal Microporous and Mesoporous Material 32: 111-117 .

Kercher, A.K. and Nagle, D. C. (2002). Evaluation of carbonized medium density fibreboard for electrical applications. Carbon 40(8): 1321-1330.

Kristin F., Felix B., WilhelmR. and Bernd M. S. (2014). Investigation of the microstructure of disordered, non-graphitic carbons by an advanced analysis method for wide- angle X-ray scattering. J. Inorganic Chemistry, 640 (15):3107-3117.

Kim K. (2001). 0101 Electrochemencycl-electrochem uses carbon. http://electrochem.cwrv.edu/ed. encycl [Accessed in June 2015].

Lam E. and Luong, J. H. (2014). Carbon materials as catalystsand catalysts supports in the transformation of biomass to fuels and chemicals," ACS Catalysis, 4:3393-33410.

Lu, Y., Li, D., Huang, X., Picard, D., Mollaabbasi, R., Ollevier, T. and Alamdari, H. (2020). Synthesis and Characterization of Bio-pitch from Bio-oil. ACSs SustainableChem. Eng. 8:11772-11782.

Pandolfo, A. G. and A.F. Hollenkamp, A. F. (2006). Carbon properties and their role in super capacitors. J. Power Sources 157: 11-27.

Rashidi, N.A. and Yusup, S. (2017). A review on recent technological advancement in the activated carbon production from oil palm wastes. Chemical Engineering Journal and the Biochemical Engineering Journal, 314:277-290.

Saeed M., Hossein K. and Ali V. (2010). Comparison of mechanical properties of date palm fiber polyethyliene composite. BioResouces, 5(4):2391-2403.

Sharukh K., Vivek P., Vikrant V. P.and Vijay K. (2015). Biomass as renewable energy. International Advanced Research Journal in Science, Engineering and Technology (IARJSET). 2(1):301-304.

Song D.,Yang C., Zhang X., Su X. and Zhang X. (2011). Structure of the organic crystallite unit in coal as determined by X-ray diffraction. Mining Science and Technology (China), 21(5):667-671.

Tang H., Mohamad D., Mohd. H.i, Ramli O. Astimar A., Abubaker E., Yap Y., Julia T. Masliana M. and Mazliza M. (2005). Electrical carbon brush from fibers of oil palm empty fruit bunch. J.Solid St. Sci. Technology letters, 12(1, 2): 45-53 .

Wang, C., Luo, Z, Li, S. and Zhu, X. 2020.Coupling effect of condensing temperature and residence time on bio-oil component enrichment during the condensation of biomass pyrolysis vapors. Fuel, 274:11786.

Yakout, S. M. and El-Deen, G. S., (2016). Characterization of activated carbon prepared by phosphoric acid activation of olive stones. Arabian Journal of Chemistry,9: S1155-S1162 .

Yan L., Chouw N., Huang L. and Kasal B. (2016). Effect of alkali treatment on microstructureand mechanical properties of coir fibers, coir fiber reinforcedpolymercomposites and reinforced-cementations composites. Constr. Build. Mater. 112:168–182.

Zhang, D.; Liu, S.; Fu, X.; Jia, S.; Min, C.; Pan, Z. (2019). Adsorption and desorption behaviors of nitrous oxide on various rank coals: Implications for oxy-coal combustion flue gas sequestration in deep coal seams. Energy Fuels, 33:11494-11506.

Doi: doi.org/10.52132/Ajrsp.en.2023.45.1